Arab J Sci Eng (2016) 41:1867–1882
DOI 10.1007/s13369-015-1998-x

RESEARCH ARTICLE - MECHANICAL ENGINEERING

The Numerical Simulation of Double-Diffusive Mixed Convection Flow in a Lid-Driven Porous Cavity with Magnetohydrodynamic Effect

C. G. Mohan[1] · **A. Satheesh**[1]

Received: 24 March 2015 / Accepted: 1 December 2015 / Published online: 28 December 2015

Abstract In this paper, the numerical investigation of double-diffusive mixed convection with magnetohydrodynamic flow in an enclosed cavity is presented. The uniform temperature and concentration are imposed along the vertical walls and the horizontal walls which are considered as insulated. The flow behaviour is analysed for two different conditions. In first case, the top wall moves towards left at a constant velocity (U_o), while the other walls remain stationary. In the second case, the top wall moves towards right with constant velocity (U_o), while the other walls remain stationary. The convective flux in the transport equations is discretized using finite volume technique with third-order deferred quadratic upwind interpolation for convection kinematics scheme at the inner nodes and the second-order central difference scheme at the outer nodes. The pressure and velocity terms are coupled by SIMPLE algorithm. The present numerical simulation is compared with the reported literature and is found to be in good agreement. The Hartmann number ($1 \leq Ha \leq 25$), Lewis number ($1 \leq Le \leq 50$) and aspect ratio ($1 \leq A \leq 2$) are varied over a wide range to analyse the non-dimensional horizontal (U) and vertical velocities (V), stream line contours, temperature and concentration gradients. The present analysis is carried out at constant Buoyancy ratio ($N = 1$) and Prandtl ($Pr = 0.7$), Richardson ($Ri = 1.0$), Darcy ($Da = 1.0$) and Reynolds ($Re = 100$) numbers. The effect of Ha, Le and A on the average Nusselt (Nu) and Sherwood (Sh) numbers is also presented.

Keywords Double-diffusive · Magnetohydrodynamic effect · Mixed convection · Hartmann number

✉ A. Satheesh
egsatheesh@gmail.com; satheesh.a@vit.ac.in

[1] School of Mechanical and Building Sciences, VIT University, Vellore, Tamil Nadu, 632014, India

Abbreviations

A	Aspect ratio
B_o	Magnetic induction (tesla)
C	Concentration
D	Mass diffusivity (m^2s^{-1})
Da	Darcy number (K/L^2)
F_c	Geometric function
g	Gravitational acceleration (ms^{-2})
Gr_C	Grashof number ($= g\beta_C \Delta C L^3/\nu^2$)
Gr_T	Grashof number ($= g\beta_T \Delta T L^3/\nu^2$)
h_s	Mass transfer coefficient (ms^{-1})
H	Enclosure height (m)
Ha	Hartmann number
k	Thermal conductivity ($Wm^{-1}K^{-1}$)
K	Permeability (m^2)
L	Enclosure length (m)
Le	Lewis number ($= Sc/Pr$)
N	Buoyancy ratio ($= Gr_T/Gr_C$)
Nu	Nusselt number ($= hL/k$)
P	Dimensionless pressure ($= pH^2/\rho\nu^2$)
Pr	Prandtl number ($= \nu/\alpha$)
Re	Reynolds number ($= V_o L/\nu$)
Ri	Richardson number (Gr_T/Re^2)
Sc	Schmidt number ($= \nu/D$)
Sh	Sherwood number ($= h_s L/D$)
T	Dimensional temperature (K)
U, V	Dimensionless velocity components along x and y axes ($= u/V_o$)
X, Y	Dimensionless Cartesian coordinates ($= x/H$)

Greek Symbols

α	Thermal diffusivity (m^2s^{-1})
β	Fluid thermal expansion coefficient (K^{-1})
θ	Dimensionless temperature ($T - T_C/T_H - T_C$)

μ Effective dynamic viscocity (Pa-s)
ν Effective kinematic viscocity (m^2s^{-1})
ρ Local fluid density (kgm^{-3})
ρ_o Fluid density at bottom surface (kgm^{-3})
ε Porosity
σ Fluid electrical conductivity ($Wm^{-1}K^{-1}$)

Subscripts

avg Average
C Cold, concentration
f Fluid
H Hot
T Temperature
L Low

1 Introduction

Double-diffusive mixed convection flow with magnetohydrodynamic effect in fluid-saturated porous media enclosed in a square cavity is gaining significance in many engineering applications [1]. Such a MHD problem is the basis of several practical applications from designing a heat exchanger and cooling the nuclear reactors, etc. Such type of applications is expected to define the future technological advancements in all engineering sectors. Magnetohydrodynamics is a branch of science that deals with the interaction of magnetic field with a fluid that conducts electricity. This can be used to alter the rate of fluid transports in the porous media as well as control its flow. Khanafer and Al-Amiri [1,2] used a two-dimensional annulus cavity to study double-diffusive mixed convective flow using Galerkin weighted residual method for solving the set of algebraic equations. Their investigation in cylindrical geometry was later expanded to mixed convection in a square cavity with the top wall moving towards right. Non-dimensional parameters were varied, and the Nusselt and Sherwood numbers were analysed.

Internal heat generation with a Darcian fluid-saturated porous media was examined for a mixed convection flow in a lid-driven cavity by Khanafer and Chamkha [3]. Alternating direct implicit procedure was used with the finite volume approach to solve the non-dimensional governing equations. Periodic behaviour by use of vibrating lid in a rectangular cavity was analysed by Chen and Cheng [4]. Pekmen and

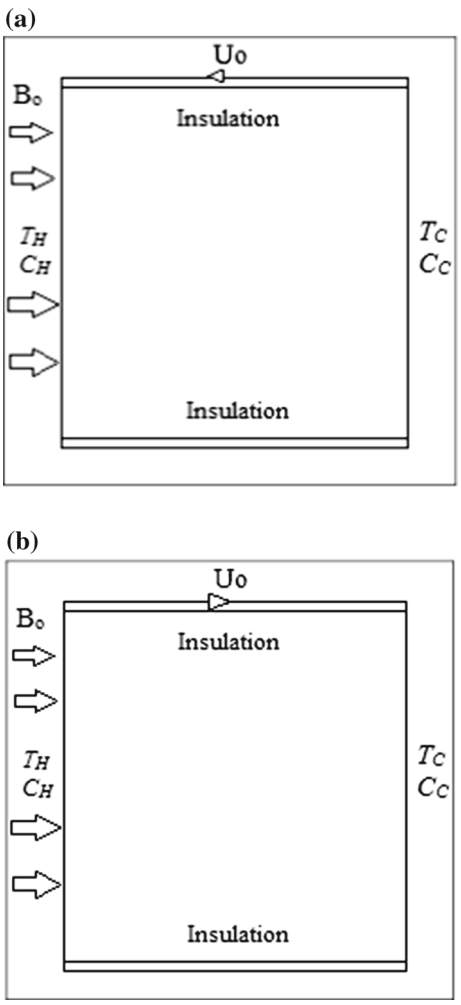

Fig. 1 Schematic of physical problem. **a** Top wall moving towards *left* direction (opposing). **b** Top wall moving towards *right* direction (aiding)

Table 1 Boundary conditions for the physical problem

Boundary conditions	T	C	U	V
Left wall ($X = 0; 0 \le Y \le 1.0$)	T_H	C_H	0	0
Right wall ($X = L; 0 \le Y \le 1.0$)	T_C	C_C	0	0
Top wall ($0 \le X \le 1.0; Y = L$)	$\frac{\partial\theta}{\partial Y} = 0$	$\frac{\partial C}{\partial Y} = 0$	−1/+1*	0
Bottom wall ($0 \le X \le 1.0; Y = 0$)	$\frac{\partial\theta}{\partial Y} = 0$	$\frac{\partial C}{\partial Y} = 0$	0	0

*Case 1/case 2

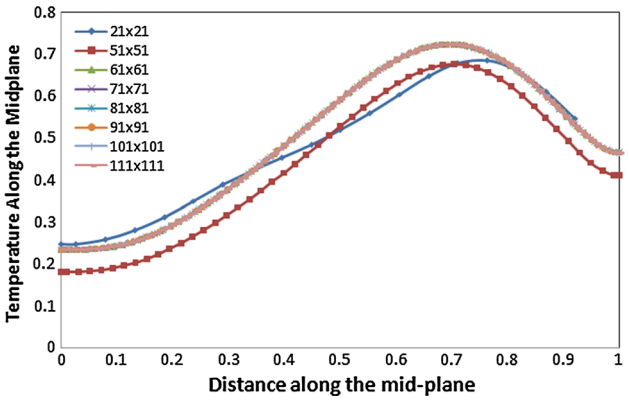

Fig. 2 Grid independent test for temperature along the mid-plane for $A = 1$, $Le = 1.0$; $Ri = 0.1$ and $Ha = 1.0$

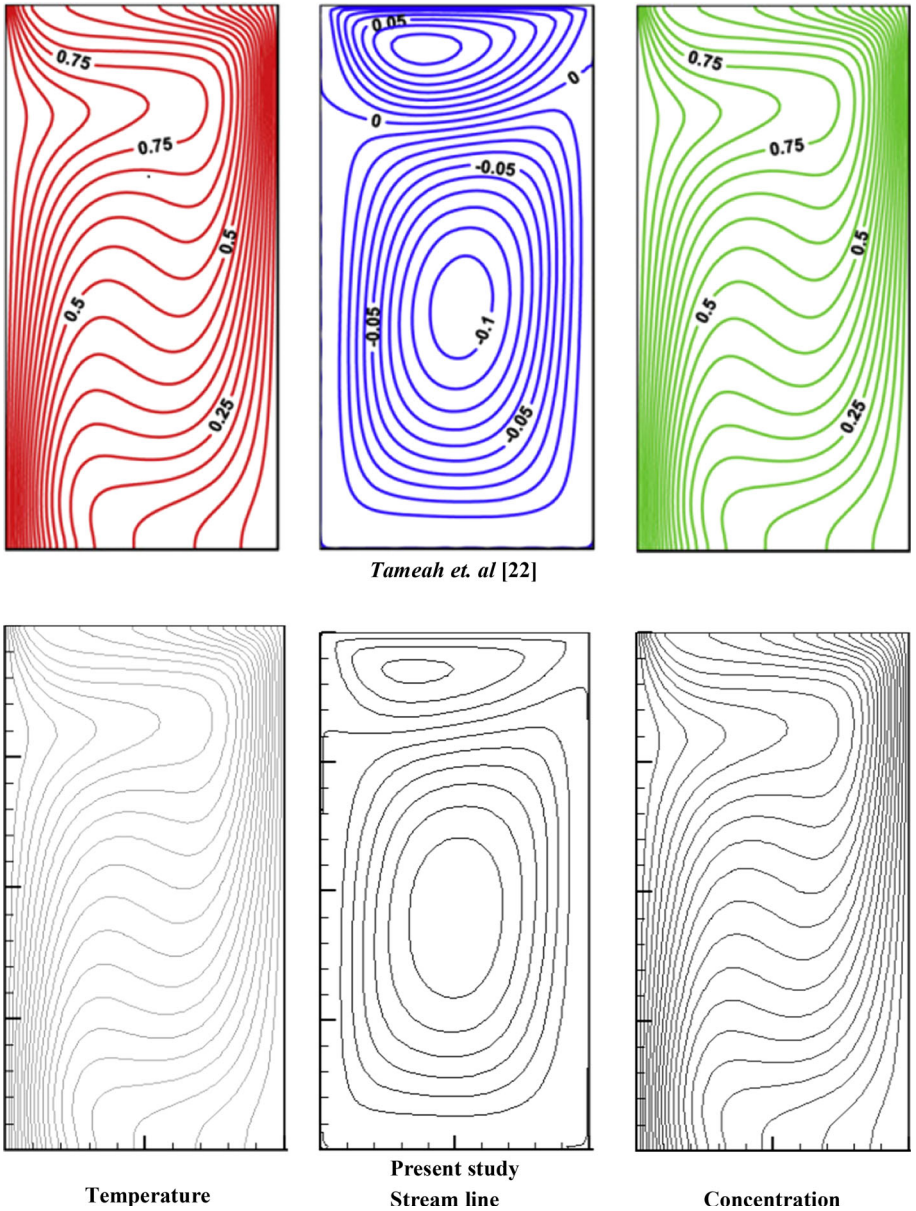

Fig. 3 Validation of numerical results with Teamah and Maghlany [22] for $Le = 1$, $Pr = 0.7$ and $N = 1$

Tezer [5] used a combination of dual reciprocity boundary element method with Houbolt scheme for solving the mixed convective MHD flow problems. They have also discussed the effects of magnetic Reynolds, Grashof, Darcy and Hartmann numbers at final steady state of the cavity. Lo [6] applied differential quadrature method to simulate transverse magnetic fields in MHD free convection flows. Bian et al. [7] found that the temperature and the velocity are modified for free convective fluid flows under the influence of magnetic field. A free convection was subjected to magnetic field induced by two electric currents and solved using finite element method with sensitive relaxation parameters which resulted in reduction in heat transfer as concluded by Costa et al. [8]. The effect of Prandtl number on MHD mixed convection was studied by Hasanpour et al. [9]. Nield [10] studied the Darcy flow in isotropic porous medium and in anisotropic medium under the effect of magnetic field. Rashad and Bakier [11] studied the effects on laminar flow of magnetic field on non-Darcy boundary layer with uniform heat flux and graphically discussed the velocity, temperature, Nusselt number and skin friction by varying parameters. Teamah and Maghlany [12] studied the effects of magnetic field in the augmentation of natural convection in a square cavity filled with nano fluids. The addition of nanoparticles was necessary to enhance the heat transfer for weak magnetic field applications, but of strong magnetic field applications there is no need for nanoparticles because the heat transfer would be decreased. They have also studied the natural convection in an rectan-

gular cavity under the influence of magnetic field and heat source [13,14].

Qasim [15] studied the combined effect of heat and mass transfer in Jeffery fluid over a stretching sheet in the presence of heat source and heat sink. Nadeem et al. [16] presented magnetohydrodynamic Casson fluid flow in two lateral directions past a porous linear stretching sheet. Hussain [17] investigated the mixed convection in a two-sided antiparallel differentially heated parallelogram cavity with the presence of magnetic field. The heat and mass transfer characteristics of air were studied with different inclination angles ($-60° \leq \Phi \leq 60°$), Hartmann numbers (0–75) and Richardson numbers (0.01–100). Misra et al. [18] presented the double-diffusive mixed convection flow in impermeable enclosed cavities without considering the effect of magnetic field to analyse the flow behaviour by varying the Lewis number and aspect ratio. The results show that the fluid flow and heat transfer increased with Le and at low aspect ratio. Rahman et al. [19] studied the mixed convection flow in a channel with a fully or partially heated cavity with the effect of magnetohydrodynamic. It was observed that the flow velocity is reduced with increase in Hartmann number, and this reduces the flow strength and heat transfer. Shit and Roy [20] investigated the effect of channel inclination on the peristaltic flow of a couple stress fluid in the presence of externally applied magnetic field. Recently, Kefayati [21] have performed the mesoscopic simulation of magnetic

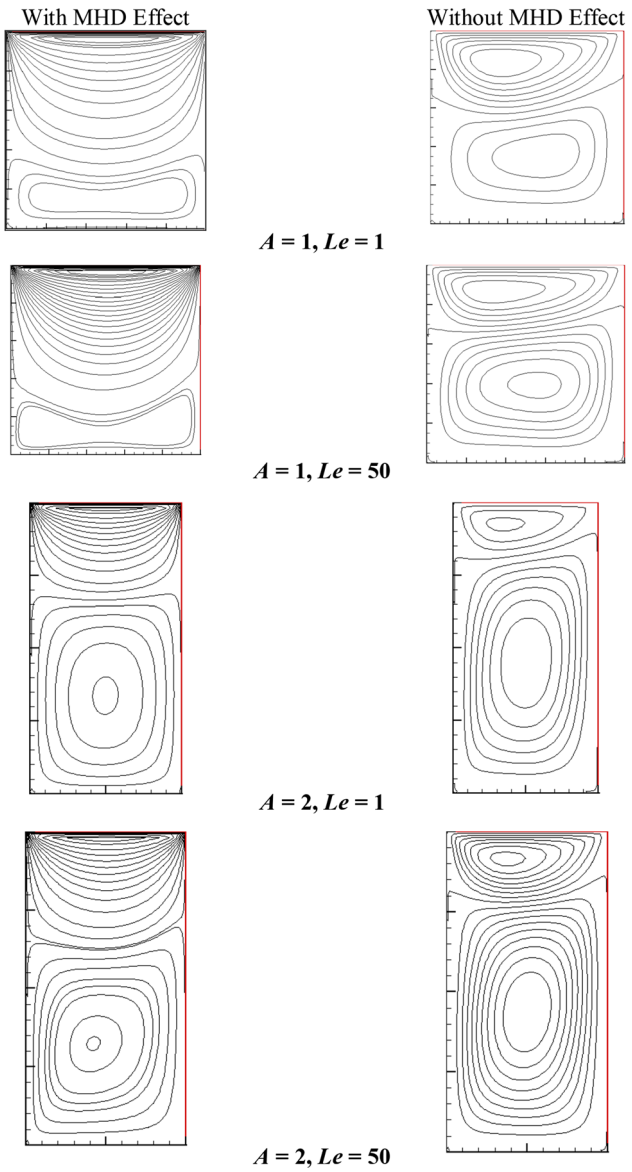

Fig. 4 Effect of magnetic field for $Ha = 10$ on the streamline flow for top wall moving *left*

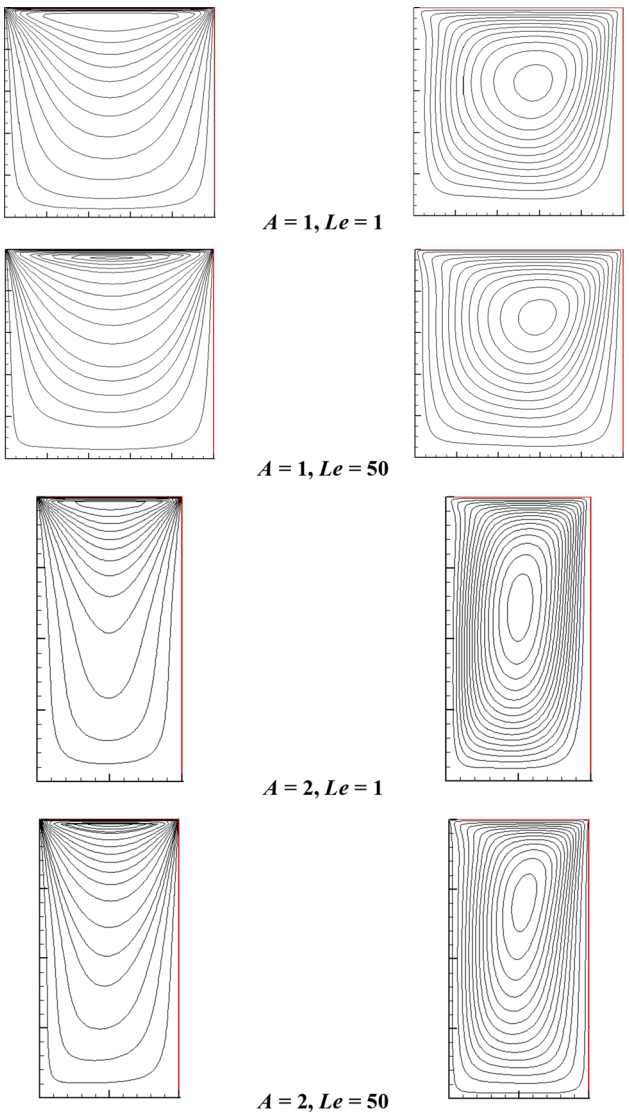

Fig. 5 Effect of magnetic field for $Ha = 10$ on the streamline flow for top wall moving *right*

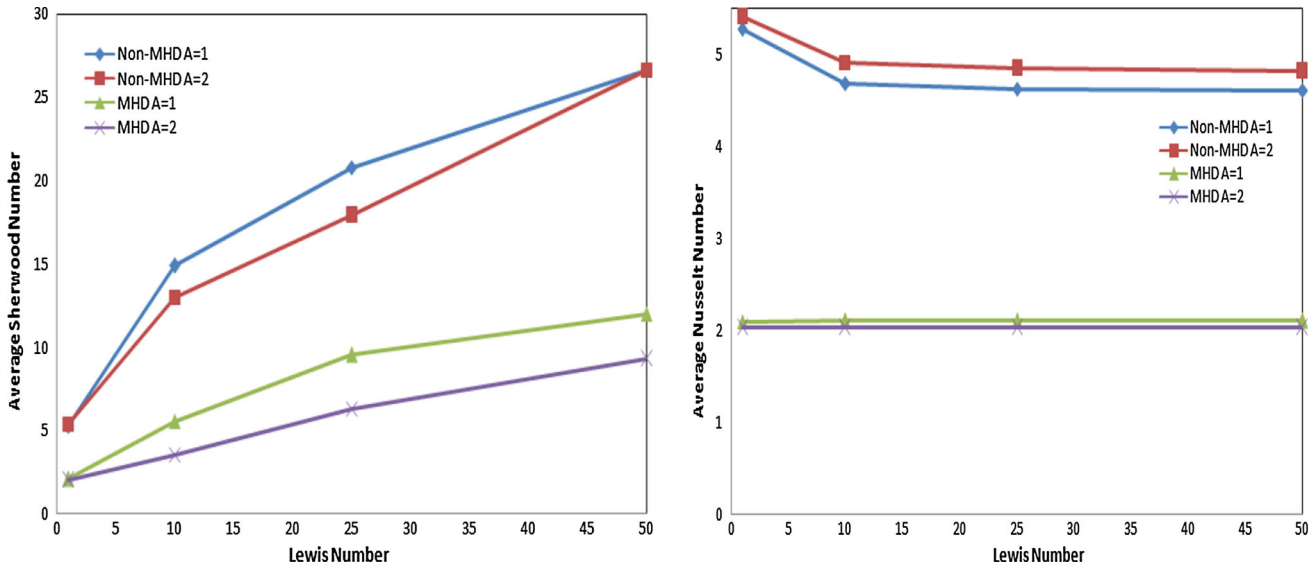

Fig. 6 Effect of magnetohydrodynamics on average Nusselt number and average Sherwood number with top moving *left*

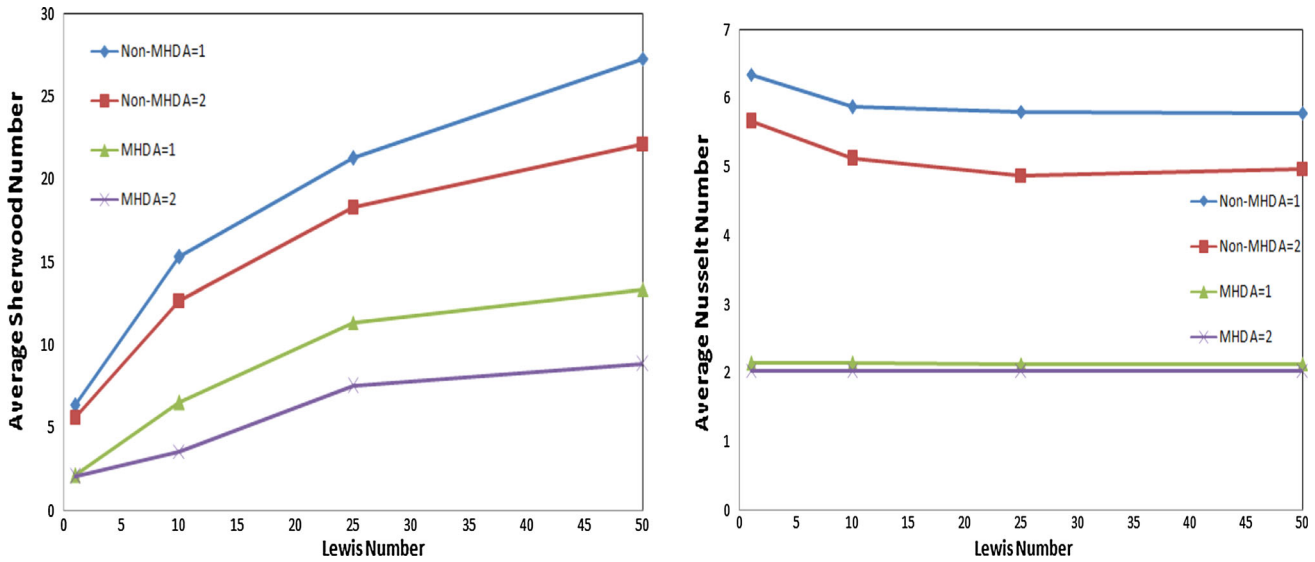

Fig. 7 Effect of magnetohydrodynamics on average Nusselt number and average Sherwood number with top moving *right*

field effect on double-diffusive mixed convection of shear-thinning fluids in a square two-sided lid-driven cavity using finite difference lattice Boltzmann method. The results show that the augmentation of Richardson number decreases heat and mass transfer and enhancement of Hartmann number opposes heat and mass transfer for different buoyancy ratios and power-law indexes. It is observed from the literature that there is a further scope of MHD flows in various engineering fields. Hence, in the present investigation authors are attempted to study the MHD mixed convection fluid flows in a porous media by varying Hartmann and Lewis numbers for different aspect ratios.

2 Mathematical Modelling and Numerical Solution

Figure 1 illustrates the two-dimensional square cavity consisting of four walls. Left and right walls are kept at constant temperature and concentration. Forced convection is provided by moving the top wall towards left (in case 1) and right (in case 2), respectively, with velocity (U_o) in x direction. The right wall is at low temperature (T_C) and low concentration (C_C), while the left wall is at high temperature (T_H) and high concentration (C_H). The magnetic field (B_o) is applied along the positive x direction from the left wall. The top and bottom walls are thermally insulated. Table 1 shows the boundary conditions considered for the present numerical model.

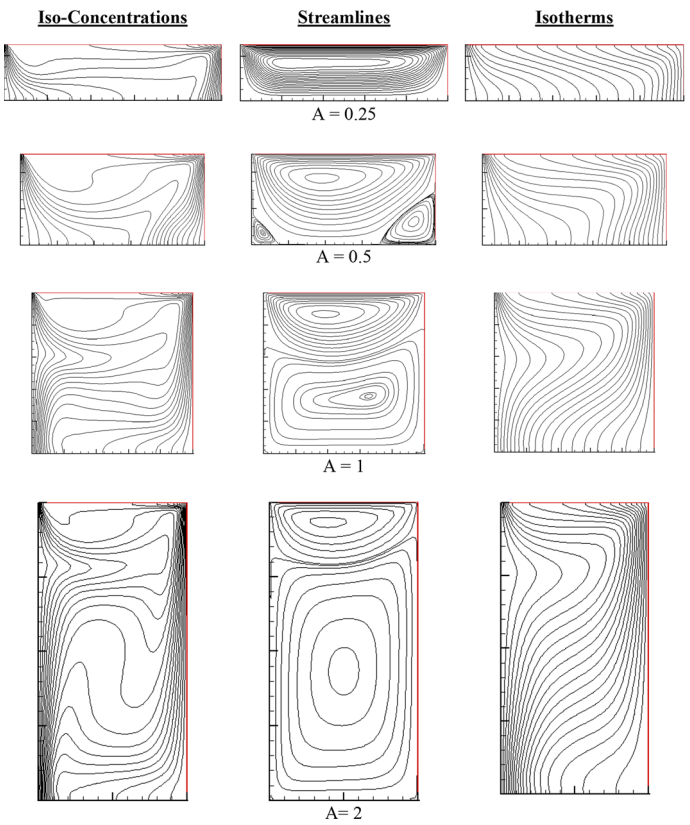

Fig. 8 Comparison of varying aspect ratios for $Ha = 1$, $Pr = 0.7$ and $Ri = 1$ top wall moving *left*

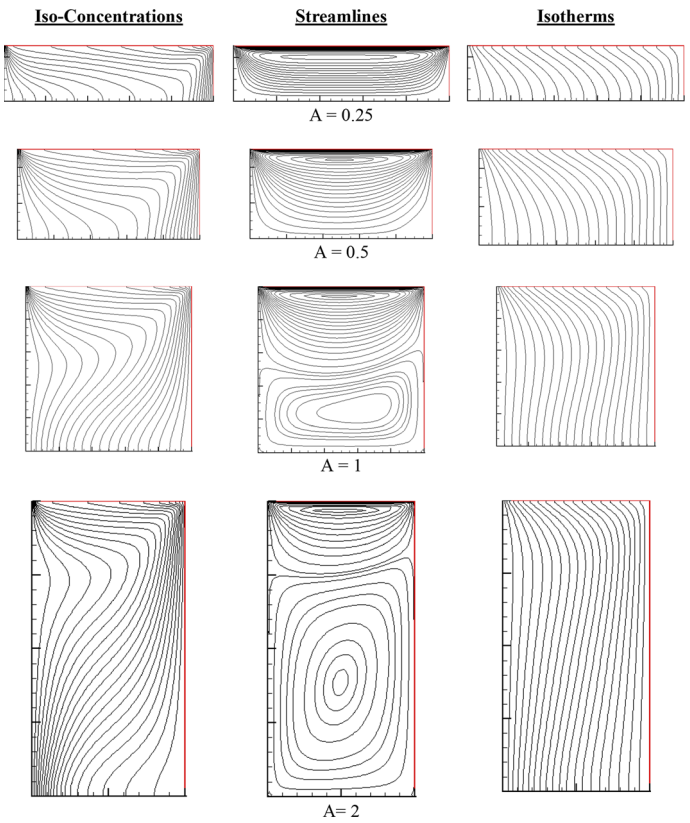

Fig. 9 Comparison of varying aspect ratios for $Ha = 5$, $Pr = 0.7$ and $Ri = 1$ top wall moving *left*

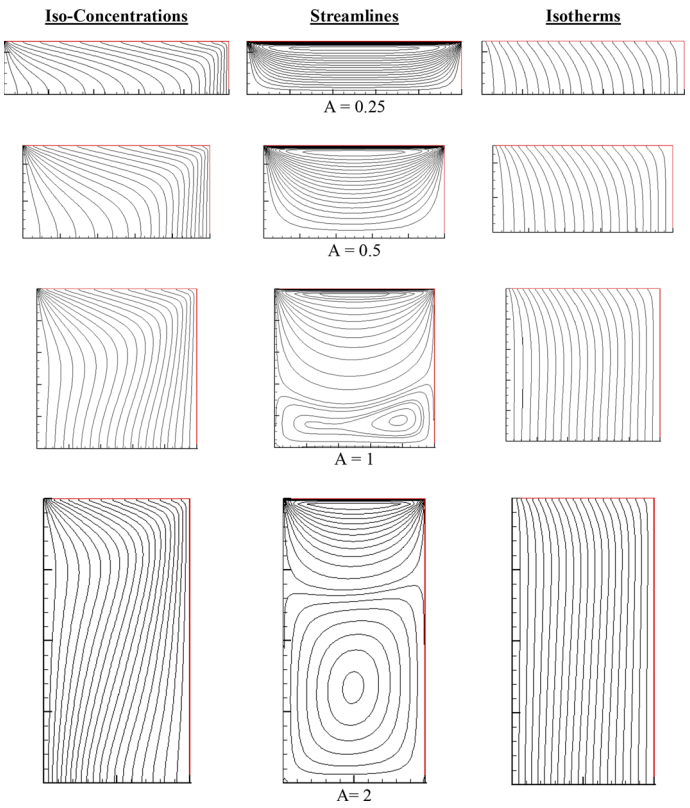

Fig. 10 Comparison of varying aspect ratios for Ha = 10, $Pr = 0.7$ and $Ri = 1$ top wall moving *left*

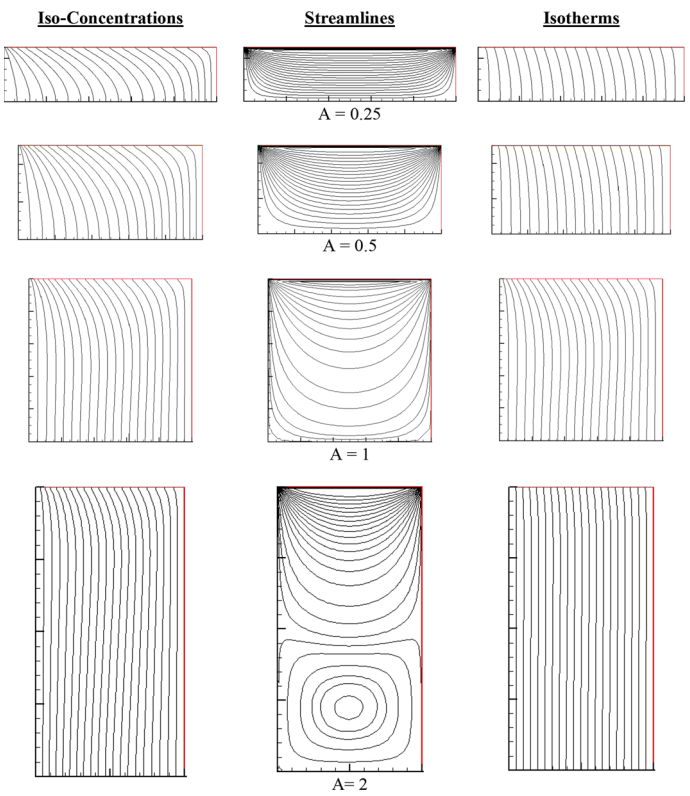

Fig. 11 Comparison of varying aspect ratios for $Ha = 25$, $Pr = 0.7$ and $Ri = 1$ top wall moving *left*

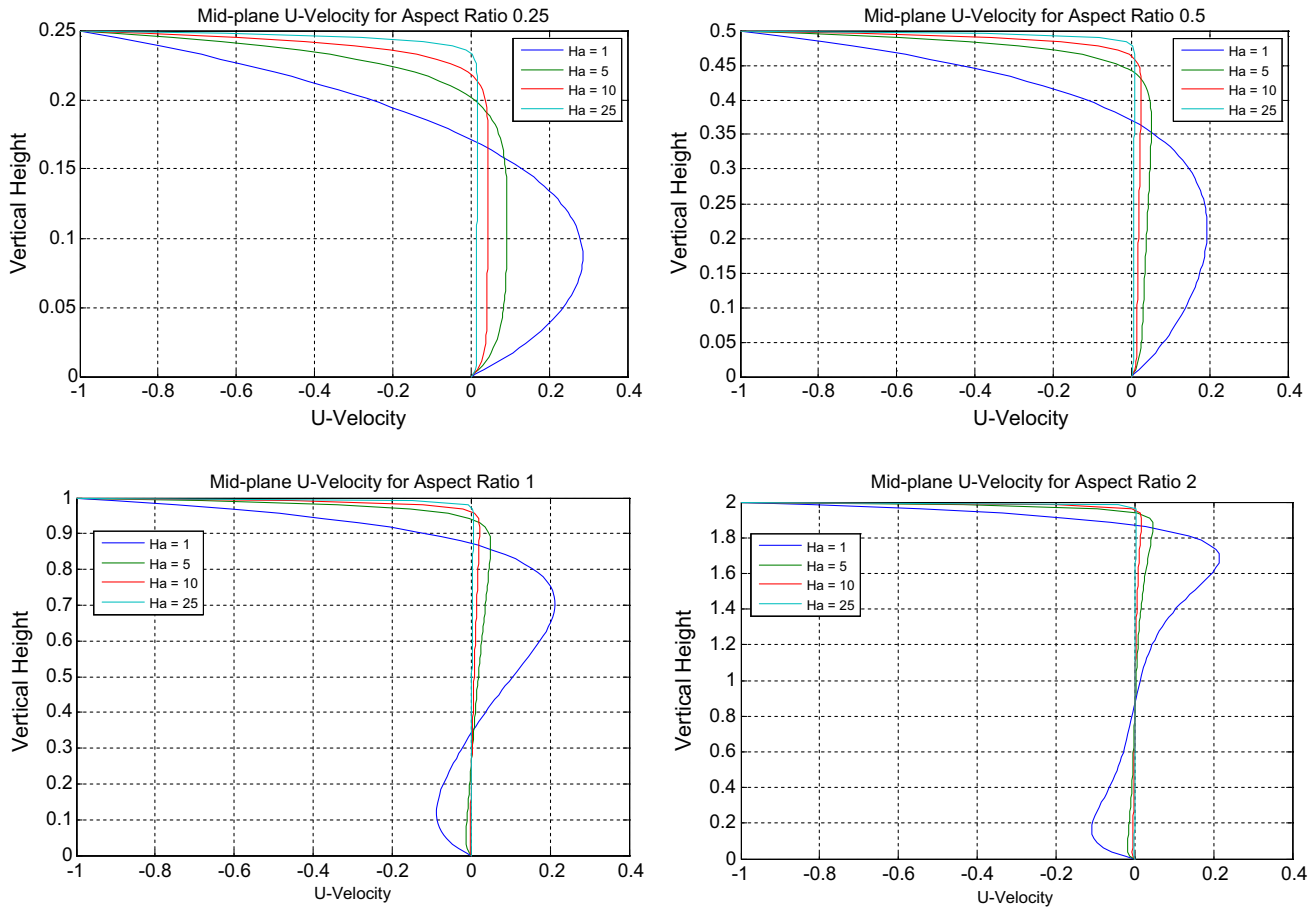

Fig. 12 Effects on Hartmann number at different aspect ratios in mid-plane U-velocity

The cavity is filled with incompressible Newtonian fluid. The fluidic porous media inside the cavity is assumed to be homogenous, isotropic and in the state of thermodynamic equilibrium. The properties of the fluid such as thermal conductivity and diffusivity are kept constant except density because of the buoyancy and magnetic effect. The density calculated from the Boussinesq approximation is as follows,

$$\rho = \rho_o \left[1 - \beta_T \left(T - T_L\right) - \beta_C \left(C - C_L\right)\right] \tag{1}$$

where,

$$\beta_T = -\frac{1}{\rho_o}\left(\frac{\partial \rho}{\partial T}\right)_{P,C} \quad \beta_C = -\frac{1}{\rho_o}\left(\frac{\partial \rho}{\partial C}\right)_{P,T}. \tag{2}$$

The governing equations for laminar, steady, two-dimensional mixed convection, after invoking Boussinesq approximation and neglecting the viscous dissipation, can be expressed in the non-dimensional form as

$$\frac{\partial U}{\partial X} + \frac{\partial V}{\partial Y} = 0 \tag{3}$$

$$\frac{1}{\varepsilon^2}\left[U\frac{\partial U}{\partial X} + V\frac{\partial U}{\partial Y}\right] = -\frac{\partial P}{\partial X} + \frac{1}{\varepsilon Re}\left(\frac{\partial^2 U}{\partial X^2} + \frac{\partial^2 U}{\partial Y^2}\right) - \frac{1}{Da\,Re}U - \frac{F_c}{\sqrt{Da}}U\sqrt{U^2+V^2} \tag{4}$$

$$\frac{1}{\varepsilon^2}\left[U\frac{\partial V}{\partial X} + V\frac{\partial V}{\partial Y}\right] = -\frac{\partial P}{\partial Y} + \frac{1}{\varepsilon Re}\left(\frac{\partial^2 V}{\partial X^2} + \frac{\partial^2 V}{\partial Y^2}\right) + \frac{Gr}{Re^2}(\theta + NC) - \frac{1}{Da\,Re}V - \frac{F_c}{\sqrt{Da}}V\sqrt{U^2+V^2} + Ha^2 PrV \tag{5}$$

$$U\frac{\partial \theta}{\partial X} + V\frac{\partial \theta}{\partial Y} = \frac{1}{RePr}\left(\frac{\partial^2 \theta}{\partial X^2} + \frac{\partial^2 \theta}{\partial Y^2}\right) \tag{6}$$

$$U\frac{\partial C}{\partial X} + V\frac{\partial C}{\partial Y} = \frac{1}{ReSc}\left(\frac{\partial^2 C}{\partial X^2} + \frac{\partial^2 C}{\partial Y^2}\right) \tag{7}$$

where Reynolds number $(Re) = \frac{U_o L}{\nu}$; thermal Grashof number $(Gr_T) = \frac{g\beta_T \Delta T L^3}{\nu^2}$; solutal Grashof number $(Gr_C) = \frac{g\beta_C \Delta C L^3}{\nu^2}$; Prandtl number $(Pr) = \frac{\nu}{\alpha}$; Schmidt number $(Sc) = \frac{\nu}{D}$; buoyancy ratio $(N) = \frac{Gr_T}{Gr_C}$; Darcy number $(Da) = \frac{K}{L^2}$; and Hartmann number $Ha = B_o L\sqrt{\frac{\sigma}{\mu}}$

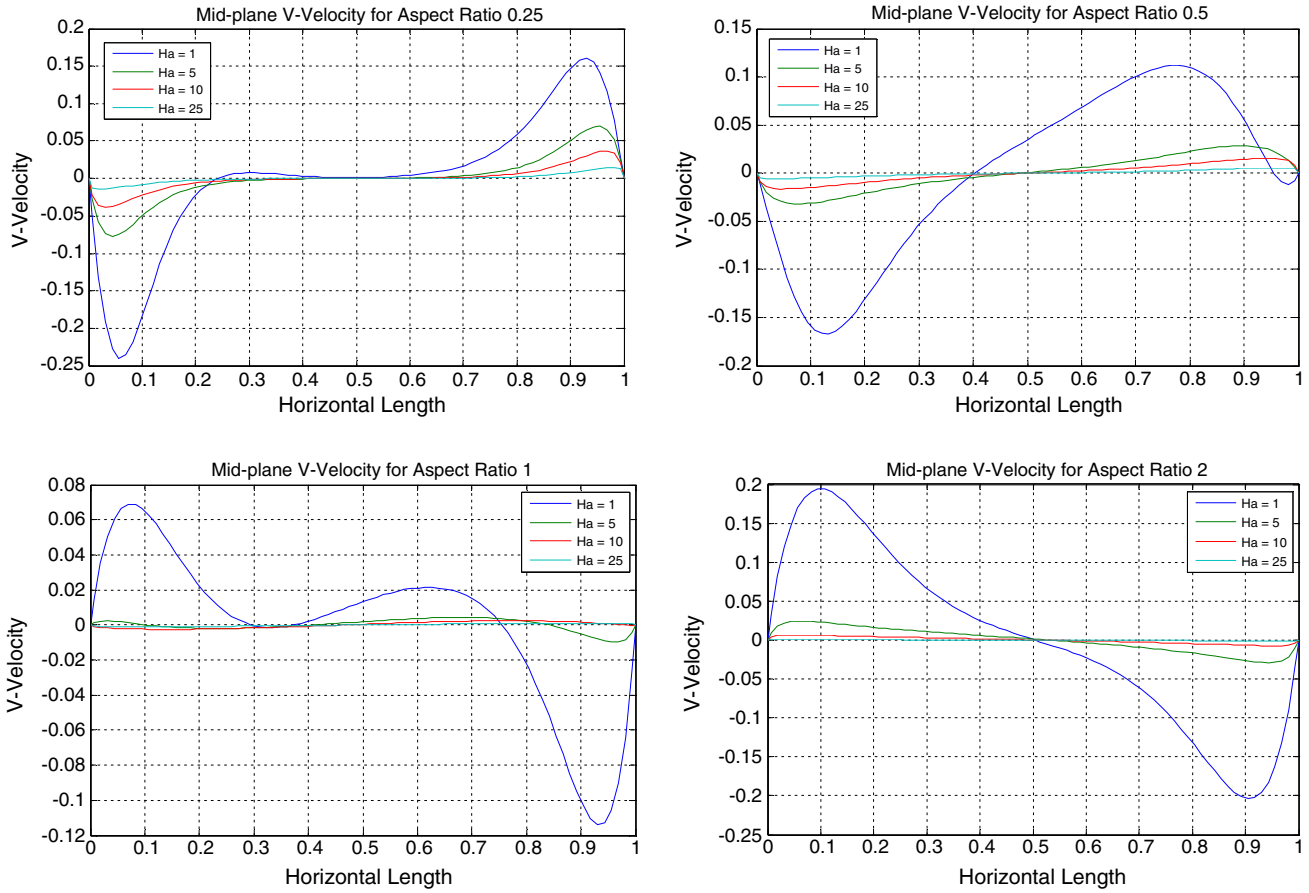

Fig. 13 Effects on Hartmann number at different aspect ratios in mid-plane V-velocity

3 Methodology

A staggered grid arrangement is used on which the governing equations are applied to obtain numerical solution using the finite volume method (FVM). A second-order central difference scheme and a third-order differed QUICK scheme are used for convection diffusion terms in the inner and outer nodes, respectively. The governing equation is numerically solved by using SIMPLE algorithm. The conservation of mass is enforced by deriving the pressure correction equation from the continuity equation. A combination of tri-diagonal matrix algorithm (TDMA) and line-by-line procedure is used to solve the discretized equations. The iterations are repeated till the following condition is satisfied,

$$\frac{\sum_i \sum_j |\Phi_{i,j}^{n+1} - \Phi_{i,j}^{n}|}{\sum_i \sum_j |\Phi_{i,j}^{n+1}|} \leq 10^{-6}.$$

where Φ denotes U, V, T and C. The subscript i and j indices denote grid locations in the x and y directions, respectively. It is observed from the present numerical results that the decrease in convergence criteria 10^{-6} does not cause any significant change in the final results.

4 Results and Discussion

Figure 2 shows the present analysis of grid independent test for mid-plane temperature. The different grids sizes of 21×21, 51×51, 61×61, 71×71, 81×81, 91×91, 101×101 and 111×111 are investigated. It is found that the values of temperature did not change after the increase in grid size from 61×61. Hence in the present numerical study, the further analysis is carried out using 61×61 grid size. In Fig. 3, the results of Teamah and Maghlany [22] are used for validation. The present FVM code results are in agreement with the literature.

4.1 Magnetohydrodynamic Effect for Top Wall Moving in Left Direction

Figures 4 and 5 show the effect of magnetic field on the flow patterns and the effect on streamline flows for top wall moving left and right, respectively. For top wall moving

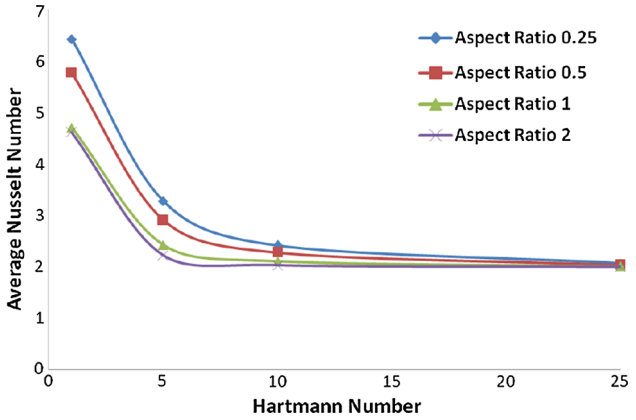

Fig. 14 Effects on average Nusselt number with varying Hartmann number

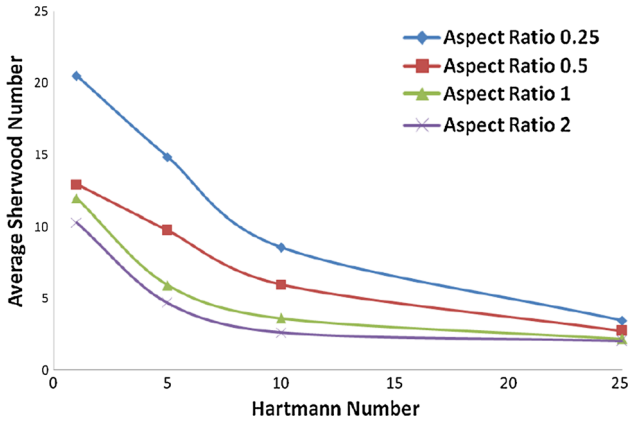

Fig. 15 Effects on average Sherwood number with varying Hartmann number

towards left, it is observed that the magnetic field aids flow for counterclockwise direction, whereas it opposes the flow for clockwise direction. It also shifts the contours towards the top for counterclockwise flows. However, it suppresses the flow patterns for clockwise direction. For the top wall moving in right, the contours are moving clockwise and shift towards the top wall, and the flow is aided by the magnetic field. Thus, it is observed that the streamline flow increases towards the top and decreases near the bottom of the cavity.

In Figures 6 and 7, we observe the shifting down of the curves when the flow is subjected to magnetic field, thereby clearly showing that magnetohydrodynamics reduces the average Nusselt number and average Sherwood number in a lid-driven cavity flow. The decrease in average Nusselt number and average Sherwood number is due to the flow decrement caused by the Hartmann number. The physical interpretation implies that when the magnetic field is applied, the drag force acts on the fluid, thereby reducing the velocity. This reduction in fluid velocity leads to reduction in heat and mass transfer along the vertical walls. This further results in lowering the average Nusselt number and average Sherwood number, and this is clearly observed from Figs. 6 and 7.

In Figs. 8, 9, 10 and 11, with increase in Ha, the effects on streamlines are observed, and it can be clearly seen that the flow patterns become more and more concentrated towards the top of the cavity and rarer towards the bottom. This shows more mixing of anticlockwise direction with increase for aspect ratio (A) 0.25. For aspect ratios increasing from 0.5 to 2, a progressive generation of anticlockwise top streamlines flow is observed with hot fluid. However, the lower streamlines and tertiary streamlines flowing in the clockwise direction with cold fluid are observed to be suppressed to the point of removal for aspect ratio 0.5 and reduced patterns for aspect ratio 1 and 2. Hence, with increase in Ha, the anticlockwise flow patterns become stronger and dominant in their respective regions, while clockwise flow pattern seems to be opposite in their respective flow.

The effect on isotherms and iso-concentrations clearly shows that there is difference in temperature and concentration distribution with increasing Ha. The heat transfer flow is seen to change its wavy pattern into rather linear and straight flow pattern for a given aspect ratio with respect to the increasing Hartmann number (Ha). Similar variation is also observed for iso-concentration. The flow pattern shows linear variation for high Hartmann number, and this means that the linear patterns are formed due to reduction in mixing ability of the fluid. However, while the iso-concentration retains the wavy patterns for values of Ha below 25, the iso-concentration flow patterns are straight and similar to isotherms for Hartmann number 25 and above. Result for Hartmann number above 25 is not displayed due to their similar behaviour.

Figure 12 represents the variation in u-velocity due to magnetohydrodynamic effect on different aspect ratios. The velocities change direction as the aspect ratio increases. The mid-plane u-velocity increases to a maximum positive value, then reaches back to zero as we move from bottom to top and then approaches the maximum velocity in $-x$ direction at top wall for $A = 0.25$ and 0.5. However, for $A = 1$ and 2, they become negative in the beginning, then reach zero and finally follow the similar trend there onwards as it approaches top wall. This is primarily due to secondary flow patterns formed at the lower part. For a given aspect ratio, the magnitude of u-velocities decreases with increase in Hartmann number. Figure 13 represents the variation in v-velocity due to magnetohydrodynamic effect on different aspect ratios. The v-velocity remains zero over a horizontal distance of 0.4–0.6 for aspect ratio 0.25, and this is due to large distance between left and right walls. Results show that the velocities change direction with increasing aspect ratio. This is attributed to the reversal of velocity and secondary streamlines formation near the centre and lower half. It is observed that there is a decrease in magnitude of v-velocity

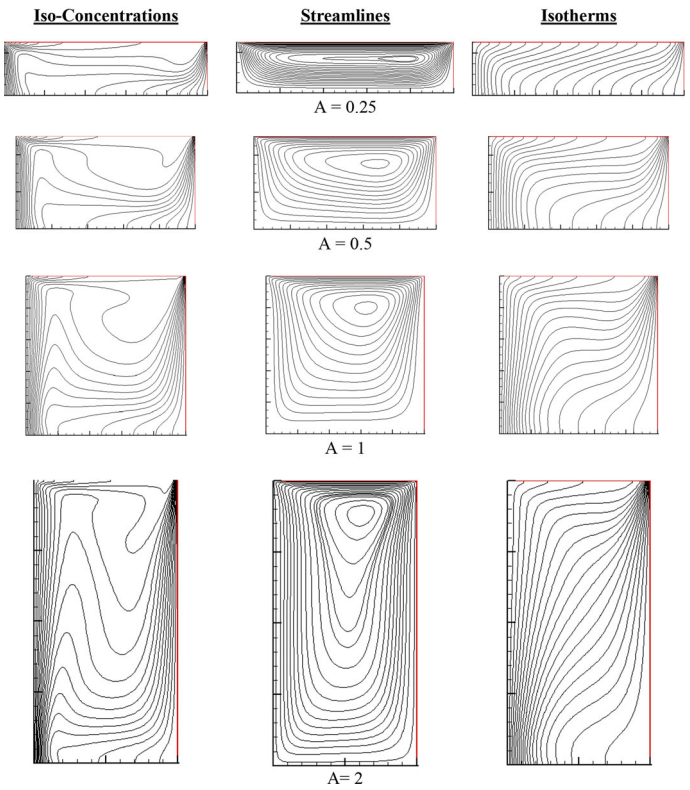

Fig. 16 Comparison of varying aspect ratios for $Ha = 1$, $Pr = 0.7$ and $Ri = 1$ top wall moving *right*

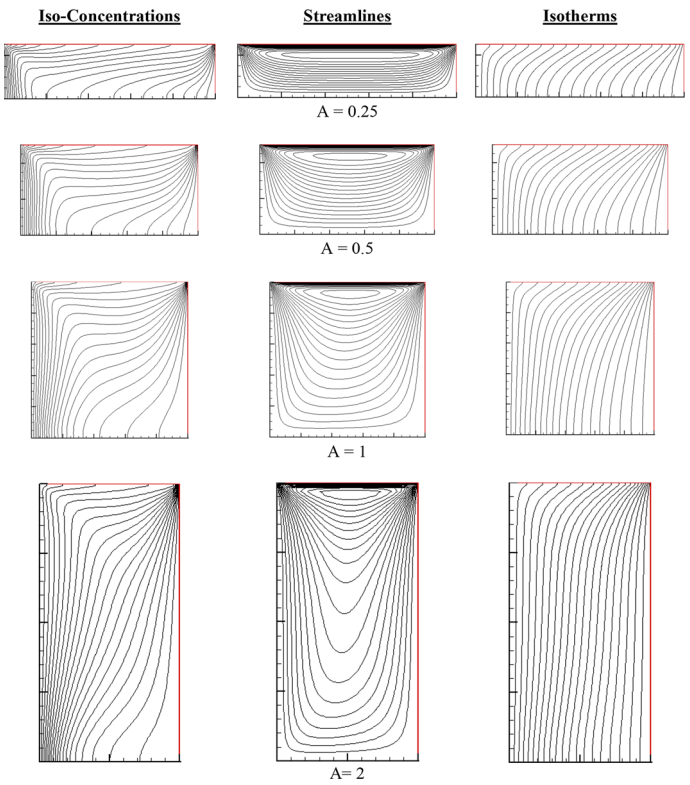

Fig. 17 Comparison of varying aspect ratios for $Ha = 5$, $Pr = 0.7$ and $Ri = 1$ top wall moving *right*

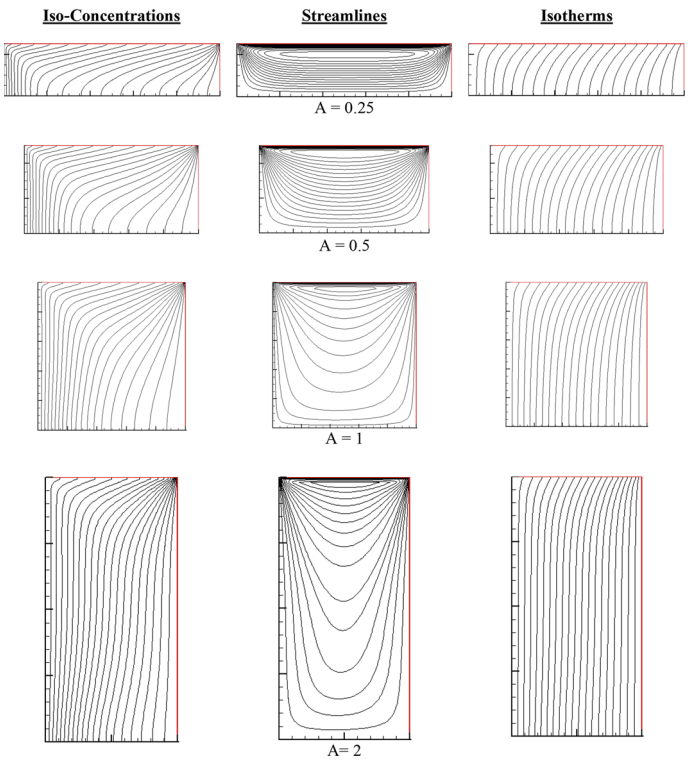

Fig. 18 Comparison of varying aspect ratios for $Ha = 10$, $Pr = 0.7$ and $Ri = 1$ top wall moving *right*

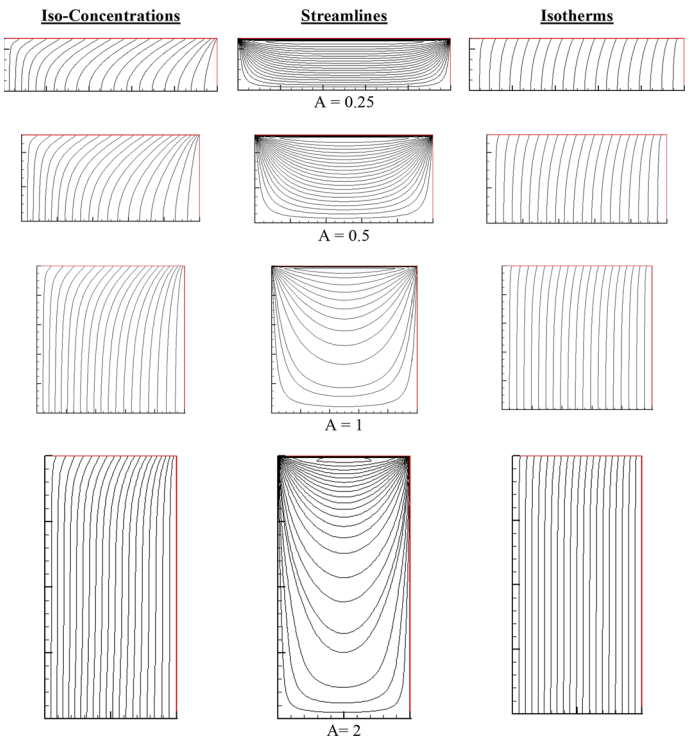

Fig. 19 Comparison of varying aspect ratios for $Ha = 25$, $Pr = 0.7$ and $Ri = 1$ top wall moving *right*

with increasing Hartmann number. Thus, we can state that as mass diffusivity decreases with increase in Hartmann number, more straight concentrations and temperature variation throughout the cavity are formed.

Figures 14 and 15 show the average Nusselt number ($\overline{Nu}$) and Sherwood number ($\overline{Sh}$) variation with respect to aspect ratio and Hartmann number. The average Sherwood number decreases with increase in Hartmann number, and it is

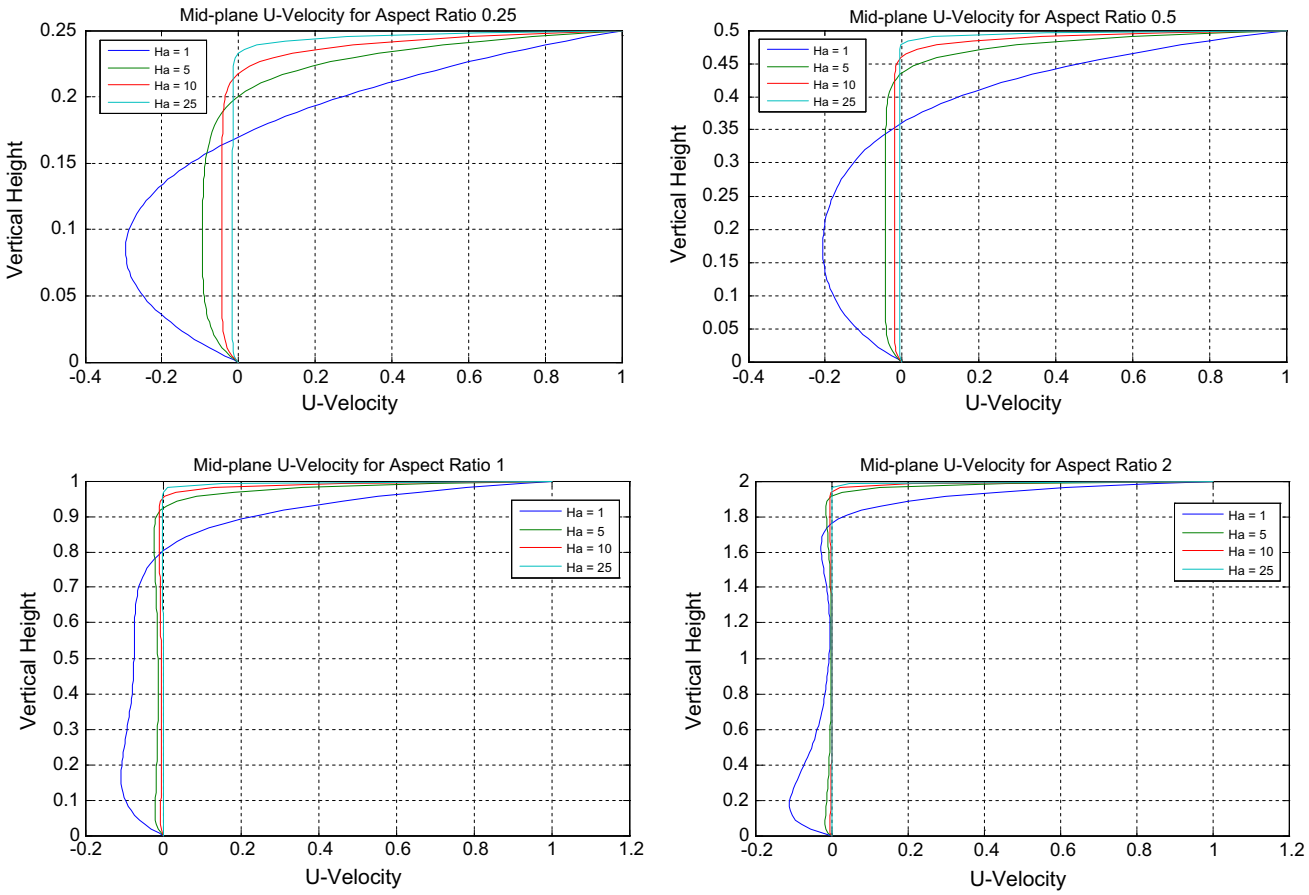

Fig. 20 Effects on Hartmann number at different aspect ratios in mid-plane U-velocity

observed that they tend to reach a point of convergence with increasing Hartmann number. This shows that mass transport is severely affected by magnetic forces. Similar behaviour is observed in the case of average Nusselt number, showing the reduction in heat transport with increment in Hartmann number. We can conclude that the magnetic forces reduce the convective heat transfer leading to further enhancement in conductive heat transport.

4.2 Magnetohydrodynamic Effect for Top Wall Moving in Right Direction

In Figs. 16, 17, 18 and 19, the effects on streamlines are observed and the flow patterns becoming more and more concentrated towards the top of the cavity and rarer towards the bottom with increase in Ha can clearly be seen. This shows that magnetic force aids the clockwise flow which is in contrast to the behaviour observed for the flow in case of top wall moving in $-x$ direction. For aspect ratios increasing from 0.5 to 2, a progressive generation of a dense clockwise top streamlines flow is observed with more mixing in the top part, whereas the lower streamlines are noted to be rarer. In the case of aspect ratio 1 and 2 especially, the fluid seems to be rather rarer in the lower part as the Hartmann number increases. The streamlines in this case do not develop a secondary streamline in the lower part as opposed to that observed with the top wall moving in left direction. However, with increase in Ha, the clockwise flow patterns become stronger and dominant in its respective regions and closer to the top wall. The effect on isotherms and iso-concentrations that are observed to be similar to those observed in the case of top wall moving left in the direction of flow and mixing is opposite to it. The similar change in wavy pattern to linear and straight flow of isotherms and iso-concentration patterns is observed for a given aspect ratio with the increase in Hartmann number (Ha). For Hartmann number 25, the iso-concentration flow patterns are straight and similar to isotherm flow patterns for all the varying aspect ratios.

Figure 20 represents the variation in u-velocity due to magnetohydrodynamic effect on different aspect ratios. For $A = 0.25$ and 0.5, the mid-plane u-velocity decreases to a minimum value, then reaches back to zero as we move from bottom to top and then approaches the maximum velocity in $+x$ direction at top wall. There is a slight linear dipping behaviour at $A = 1$ from height 0.2–0.7. For

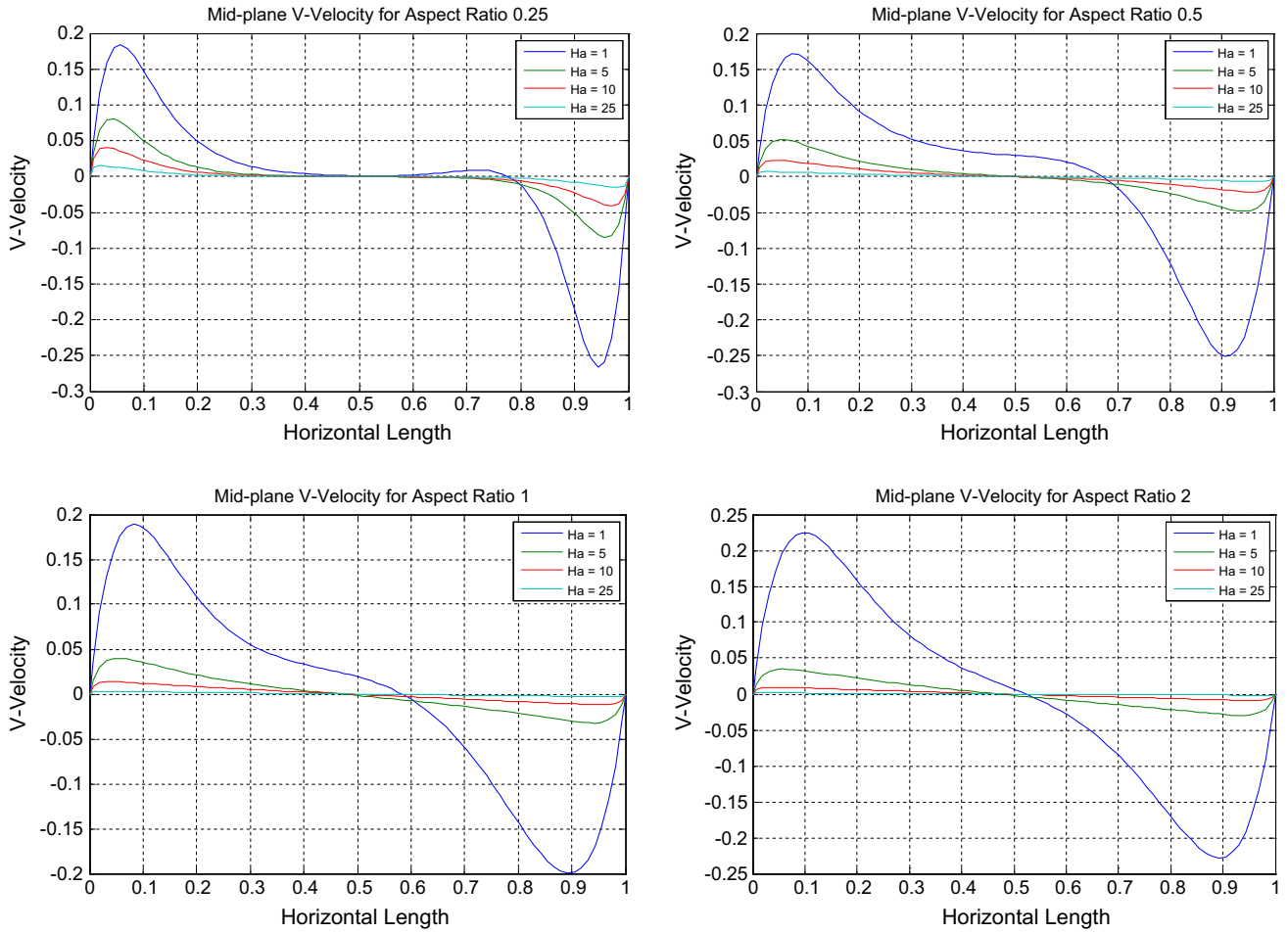

Fig. 21 Effects on Hartmann number at different aspect ratios in mid-plane V-velocity

$A = 2$, velocity is zero from height 1–1.2 and then again becomes negative till it moves to zero and further on to the maximum velocity at top wall. This is primarily due to big difference in the bottom and top wall leading to vacant space in between. For a given aspect ratio, the magnitude of u-velocities decreases with increase in Hartmann number.

Figure 21 represents the variation in v-velocity due to magnetohydrodynamic effect on different aspect ratios. For $A = 0.25$ the v-velocity remains zero over horizontal distance of 0.45–0.55, and this is due to very high distance between the left and right walls. The location of conversion of v-velocity from positive to negative is seen to move from 0.8 at $A = 0.25$ to approximately 0.55 at $A = 2$. It is also observed that there is a decrease in the magnitude of v-velocity with increase in Hartmann number. Similar to the top wall moving towards left, we can state that mass diffusivity decreases with increase in Hartmann number. Figures 22 and 23 show the average Nusselt number ($\overline{Nu}$) and Sherwood number ($\overline{Sh}$) variation with respect to Hartmann number and aspect ratio. The pattern is same as that of top wall moving in $-x$ direction; the average Sherwood number decreases with increase in Hartmann number and tends to converge with increasing Hartmann number. Nusselt number, on the other hand, is quite close to convergence at Hart-

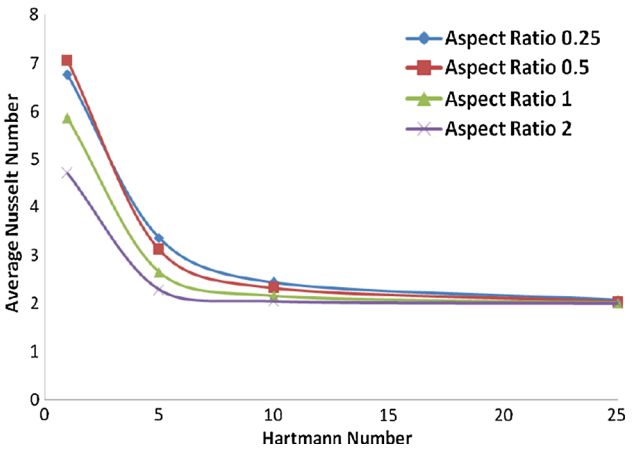

Fig. 22 Effects on average Nusselt number with varying Hartmann number

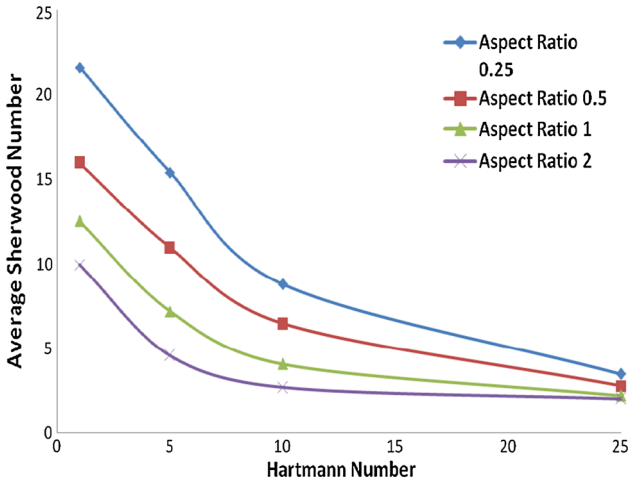

Fig. 23 Effects on average Sherwood number with varying Hartmann number

mann number 25. This shows that heat and mass transport is severely reduced by magnetic forces. Thus, the applied magnetic force seems to promote diffusive transport as opposed to convective transport when applied across a lid-driven cavity.

5 Conclusions

The fluid behaviour is investigated for a two-sided lid-driven cavity with porous nature due to double-diffusive mixed convection and magnetohydrodynamics. The effect of Hartmann number (Ha) and aspect ratio, for a fixed Lewis number, on streamline contours, temperature and concentration gradient is presented. The average Nusselt numbers and Sherwood numbers are used to represent the heat and mass diffusion. For low Hartmann numbers, the variation of u and v-velocities is found to be insignificant, but as we increase the Ha, significant decrease in their magnitudes is observed for both cases of top wall moving towards left and towards right. Results show that the fluid flow decreases with increase in Ha. The effect of magnetic field on the thermal gradient and concentration gradient has been significant for high Ha. It can be said that the fluid tends to prefer diffusive transport instead of convective transport, which is primarily due to restrictions on flow by increasing viscous nature of the fluid with increase in applied magnetic field strength. From this analysis, it is concluded that magnetohydrodynamic effect plays an important role in temperature and concentration which are function of aspect ratio and Hartmann number. The effect of magnetohydrodynamics on mixed convection is so significant that magnetic field cannot be neglected in mixed convection heat transfer problems.

References

1. Al-Amiri, A.M.: Analysis of momentum and energy transfer in a lid-driven cavity filled with a porous medium. Int. J. Heat Mass Transf. **43**(1), 3513–3527 (2000)
2. Al-Amiri, A.M.; Khanafer, K.M.; Pop, I.: Numerical simulation of combined thermal and mass transport in a square lid-driven cavity. Int. J. Therm. Sci. **46**(7), 662–671 (2007)
3. Khanafer, K.; Chamkha, A.J.: Mixed convection in a lid-driven enclosure with a fluid-saturated porous medium. Int. J. Heat Mass Transf. **42**, 2465–2481 (1999)
4. Chen, C.L.; Cheng, C.H.: Numerical simulation of periodic mixed convection heat transfer in a rectangular cavity with a vibrating lid. Appl. Therm. Eng. **29**, 2855–2862 (2009)
5. Pekmen, B.; Tezer-Sezgin, M.: MHD flow and heat transfer in a lid-driven porous enclosure. Int. J. Comput. Fluids **89**, 191–199 (2014)
6. Lo, D.C.: High-resolution simulations of magnetohydrodynamic free convection in an enclosure with transverse magnetic field using velocity–vorticity formulation. Int. Commun. Heat Mass Transf. **37**, 514–523 (2010)
7. Bian, W.; Vasseur, P.; Bilgen, E.; Meng, F.: Effect of electromagnetic field on natural convection in an inclined porous layer. Int. J. Heat Fluid Flow **17**, 36–44 (1996)
8. Costa, V.A.F.; Sousa, A.C.M.; Vasseur, P.: Natural convection in square enclosures filled with fluid-saturated porous media under the influence of the magnetic field induced by two parallel vertical electric currents. Int. J. Heat Mass Transf. **55**, 7321–7329 (2012)
9. Hasanpour, A.; Farhadi, M.; Sedighi, K.; Ashorynejad, H.R.: Numerical study of Prandtl effect on MHD flow at a lid-driven porous cavity. Int. J. Numer. Methods Fluids **70**, 886–898 (2012)
10. Nield, D.A.: Modelling the effects of a magnetic field or rotation on flow in a porous medium momentum equation and anisotropic permeability analogy. Int. J. Heat Mass Transf. **42**, 3715–3718 (1999)
11. Rashad, A.M.; Bakier, A.Y.: MHD effects on non-Darcy forced convection boundary layer flow past a permeable wedge in porous medium with uniform heat flow. Nonlinear Anal. Model. Control **14**(2), 249–261 (2009)
12. Teamah, M.A.; El-Maghlany, W.M.: Augmentation of natural convective heat transfer in square cavity by utilizing nanofluids in the presence of magnetic field and uniform heat generation/absorption. Int. J. Therm. Sci. **58**, 130–142 (2012)
13. Teamah, M.A.: Numerical simulation of double diffusive natural convection in rectangular enclosure in the presences of magnetic field and heat source. Int. J. Therm. Sci. **47**(3), 237–248 (2008)
14. Teamah, M.A.; Elsafty, A.F.; Massoud, E.Z.: Numerical simulation of double-diffusive natural convective flow in an inclined rectangular enclosure in the presence of magnetic field and heat source. Int. J. Therm. Sci. **52**, 161–175 (2012)
15. Qasim, M.: Heat and mass transfer in a Jeffrey fluid over a stretching sheet with heat source/sink. Alex. Eng. J. **52**(4), 571–575 (2013)
16. Nadeem, S.; Haq, R.U.; Akbar, N.S.; Khan, Z.H.: MHD three-dimensional Casson fluid flow past a porous linearly stretching sheet. Alex. Eng. J. **52**(4), 577–582 (2013)
17. Hussain, S.H.: Magnetohydrodynamics opposing mixed convection in two-sided lid-driven differentially heated parallelogrammic cavity. J. Babylon Univ./Eng. Sci. **21**(4), 1223–1242 (2013)
18. Misra, S.; Satheesh, A.; Mohan, C.G.; Padmanathan, P.: The numerical simulation of double-diffusive laminar mixed convection flow in a porous cavity. WSEAS Trans. Heat Mass Transf. **8**(4), 131–138 (2013)
19. Rahman, M.M.; Öztop, H.F.; Saidur, R.; Mekhilef, S.; Al-Salem, K.: Finite element solution of MHD mixed convection in a channel with a fully or partially heated cavity. Comput. Fluids **79**, 53–64 (2013)

20. Shit, G.C.; Roy, M.: Hydromagnetic effect on inclined peristaltic flow of a couple stress fluid. Alex. Eng. J. **53**(4), 949–958 (2014)
21. Kefayati, G.H.R.: Mesoscopic simulation of magnetic field effect on double-diffusive mixed convection of shear-thinning fluids in a two sided lid driven cavity. J. Mol. Liq. **198**, 413–429 (2014)
22. Teamah, M.A.; El-Maghlany, W.M.: Numerical simulation of double-diffusive mixed convective flow in rectangular enclosure with insulated moving lid. Int. J. Therm. Sci. **49**(9), 1625–1638 (2010)